One-hole Green function, momentum distribution and quasiparticle weight of the U to infinity 1D Hubbard model

1992 J. Phys.: Condens. Matter 4 3589

(http://iopscience.iop.org/0953-8984/4/13/020)

J. Phys.: Condens. Matter 4 (1992) 3589–3610. Printed in the UK

One-hole Green function, momentum distribution and quasiparticle weight of the $U \rightarrow \infty$ 1D Hubbard model

S Sorella† and A Parola‡

† International School for Advanced Studies, Via Beirut 2, Trieste, Italy
‡ Dipartimento di Fisica, Universitá di Milano, Via Celoria 16, 20133 Milano, Italy

Received 19 November 1991

Abstract. Starting from the known Lieb and Wu solution of the one-dimensional Hubbard model in the $U \rightarrow \infty$ limit, we show how the spin–charge decoupling of the elementary excitations is responsible for several peculiar features in one-particle properties, such as momentum distribution, quasiparticle weight and the Green function. In particular we analyse in detail the structure of the one-hole Green function at half-filling, which has not been previously calculated by field theory methods due to the breakdown of conformal invariance. A rich structure is found with branch cut singularities at $\omega = \pm 2 \sin k$ but no simple poles. The non-trivial dependence on the momentum of the hole allows for hole propagation although the analytic structure of $G(k, \omega)$ is quite different from that usually characterizing band insulators. These results provide a precise characterization of one-dimensional Mott insulators. The relationship between the branch cuts of the Green function and the finite-size scaling of the quasiparticle weight is also discussed together with its implications for the analysis of numerical data.

1. Introduction

The recent discovery of high T_c superconductors has renewed interest in Mott insulators, suggesting that the basic physics of hole dynamics in a quantum antiferromagnet is still awaiting a completely satisfactory theoretical understanding. The half-filled Hubbard model is probably the simplest realization of a Mott insulator, and, as a first step, it is natural to investigate the dynamical properties of a single hole in this model. The results might help the interpretation of photoemission experiments in real antiferromagnets and would give physical insight about the effects of doping in these materials. This problem has been a subject of study since the pioneering work of Brinkman and Rice [1] (BR) who argued that the hole motion is strongly inhibited by the frustrating effect of hopping on the antiferromagnetic ordering. Their treatment is exact in one dimension when quantum fluctuations on spin dynamics are neglected and leads to the inhibition of hole motion, but no convincing estimate on the effects of fluctuations has yet been given, even in one dimension. This is probably due to the fact that fluctuation corrections in one dimension are non-perturbative and standard diagrammatic techniques fail.

The usual one-body description of the dynamical properties of a hole can be applied to the single band Hubbard model at half-filling, provided that antiferromagnetic correlations are schematically taken into account by the creation of two effective 'Hubbard bands'. In this case, the Mott insulator becomes a conventional insulator

0953-8984/92/133589+22$04.50

where the electron density is such to fill completely the lower band, the upper being empty. When an extra particle is injected in the system (hole or an electron) it propagates like a free particle with an effective mass related to the curvature of the bands. The first-principles justification of such a picture is, however, an open problem, particularly at low dimensions where much more sophisticated theoretical approaches are required. In two dimensions the problem has been attacked in the strong coupling limit of the Hubbard model (the t–J model) [2–4], where diagrammatic self-consistent approaches and the spin-wave approximation indicate that, for finite J, the hole propagates similarly to the conventional case. The situation is more interesting for $J = 0$ (i.e. $U \rightarrow \infty$), where in the BR picture, and in the retraceable path approximation, the motion of a hole is entirely incoherent due the divergences of the one-particle density of states. Such a calculation also shows that in a classical antiferromagnetic state (Néel state) there is no dispersion for single hole excitations and therefore the hole is strictly localized in any dimension. Numerical works [5] have qualitatively confirmed this picture although a precise quantitative comparison has not been attempted and the delicate question of marginal behaviour for the hole propagation has not yet been clarified.

Due to the difficulties of these problems, it is useful to investigate this issue accurately in one dimension where it is known that at finite density of holes the system is characterized by non-conventional properties [6–14]. Exact results at finite doping have been obtained by a variety of techniques, ranging from renormalization group approaches, asymptotic expansion of the Lieb and Wu wavefunction and field theory methods. In particular, the latter route proved very fruitful, leading to the determination of critical exponents in the whole phase diagram of the model. However, both renormalization group and mapping to a field theory become singular precisely at half-filling due to the presence of a gap in the charge excitation spectrum. This prevents a direct use of these powerful methods for the characterization of hole dynamics in quantum antiferromagnets. The recently developed formalism [9–11] for the calculation of physical properties in the $U \rightarrow \infty$ Hubbard model instead appears to be the appropriate tool for investigating the dynamics of a single hole in Mott insulators.

In this paper, we present results concerning several one-particle properties of the $U \rightarrow \infty$ Hubbard model. In particular, the analytical structure of the momentum distribution at finite doping is discussed: known results, like the non-Fermi liquid nature of the system or the critical exponent of the leading singularity, are derived together with less settled features, like the presence of a sub-leading $3k_F$ singularity. Moreover the results on the momentum distributions are related to the vanishing of the quasiparticle weight in the thermodynamic limit and the form of the finite-size scaling of the quasiparticle weight is explicitly found. The *holon* contribution coming from the charge degrees of freedom and the *spinon* term, coming from spin dynamics, are identified and their dependence on the doping is discussed.

Most of the paper is, however, devoted to the study of the dynamics of one hole in the one-dimensional Hubbard model. Using some of the previously obtained results, we are able to derive an analytic expression for the one-particle Green function $G(k,\omega)$ at half-filling. All the divergences of its imaginary part as a function of momentum and frequency are exactly located in the (k,ω) plane. Numerical diagonalization in small rings is also used to show the form of the Green function far from the branch cuts and an analytical fit of $G(k,\omega)$ in the thermodynamic limit is given.

The resulting hole dynamics turns out to be strongly dependent on the choice of

the spin configuration of the half-filled Hubbard model. In fact, in one dimension and exactly at $U = \infty$ [15] all spin configurations are degenerate: If a classical, non-fluctuating Néel state is chosen, we recover the well known BR results characterized by the absence of hole propagation. However in the $U \to \infty$ limit the spin degeneracy is lifted and the ground state of the Heisenberg model is singled out. This state is characterized by strong quantum fluctuations and no long-range order. In this case the calculation of the Green function shows that the hole can propagate in such a spin background, although the scattering with spin excitations (*spinons*) leads to the suppression of the poles in the Green function which are replaced by weaker singularities (branch cuts). The physical origin of this behaviour is identified in the anomalous classification of the elementary excitations for the half-filled Hubbard model. In particular, the spin–charge decoupling turns out to be the basic feature allowing this kind of hole propagation.

2. The exact wavefunction in the $U \to \infty$ limit

The one-dimensional Hubbard model is defined by the well known Hamiltonian:

$$H = -\sum_{i,\sigma}(c^{\dagger}_{i,\sigma}c_{i+1,\sigma} + hc) + U\sum_{i} n^{\uparrow}_{i}n^{\downarrow}_{i}. \tag{2.1}$$

Lieb and Wu [16] have given a formally exact solution for the spectrum and eigenstates of the Hubbard model at any filling and, in principle, this allows the calculation of all physically interesting quantities. However this Bethe ansatz solution is unmanageable except in the $U \to \infty$ limit where the analytic structure simplifies and some correlation functions can be explicitly calculated. In this limit several authors have shown that all the eigenstates can be written in the following 'product' form:

$$\psi(x_1 \dots x_N, y_1 \dots y_M) = \psi_{SF}(x_1 \dots x_N)\phi_H(y_1 \dots y_M) \tag{2.2}$$

where $x_1 \dots x_N$ are the spatial coordinates of the N electrons on a L-site ring, and the $y_1 \dots y_M$ 'coordinates' label the positions of the spin-up electrons on the squeezed Heisenberg ring [9], i.e. on the ring whose sites are just the *occupied* sites of the Hubbard chain. ψ_{SF} is a spinless fermion state to be specified later and ϕ_H is an eigenstate of an N-site Heisenberg Hamiltonian with periodic boundary conditions. Although an exhaustive discussion of the structure of this wavefunction has been given in [9], here it is useful to stress that the product form of equation (2.2) should not be interpreted as a trivial decoupling between charge and spin. In fact, the mapping between the real chain (characterized by the x_i coordinates) and the squeezed chain (of coordinates y_i) depends on the charge configuration, that is on the set $\{x_i\}$ which specifies the position of the electrons. A noticeable exception is the half-filled Hubbard model ($N = L$) where only one charge configuration is allowed in the $U \to \infty$ limit, and the spinless fermion part of the wavefunction becomes trivial. The actual analytical evaluation of physical correlation functions with such a wavefunction is a difficult task involving the separate calculation of many-particle correlation functions of the spinless fermion gas and of the Heisenberg model, as will be shown later.

As usual, we choose an even total number of particles $N = 4n + 2$, where n is an integer and the number of spin-up electrons equals the number of spin-down ones.

In this case the ground state is a non-degenerate singlet of zero momentum. In the following, our main concern will be on single particle properties and therefore the precise structure of the ground-state wavefunction of N *and* $N-1$ electrons will be used. In particular the charge parts of both ψ^N and ψ^{N-1} are Slater determinants of plane waves, but they correspond to different choices of the allowed momenta. More precisely, the N-particle state is characterized by the wavevectors

$$k_j = \frac{2\pi}{L}(j + \tfrac{1}{2}) \tag{2.3}$$

with j ranging in the interval $[-2n-1, 2n]$ while the $N-1$ particle state has

$$k_j = \frac{2\pi}{L}\left(j + \frac{n}{4n+1}\right) \tag{2.4}$$

and now j belongs to $[-2n, 2n]$.

The energy of such a state is related only to the occupied spinless fermion levels and does not depend on the spin part of the wavefunction. This property holds at $U = \infty$ and just in one dimension where the Hamiltonian conserves the spin ordering. In this case, the explicit expression of the energy in terms of the previously defined momenta coincides with that of a free fermi gas:

$$E(\{k_j\}) = -2\sum_j \cos k_j \tag{2.5}$$

where the sum runs over the N occupied levels. Of course, the ground state corresponds to the lowest set of k_j compatible with the Pauli principle. Following [9], we also notice that the wavefunction (2.2) includes the first correction (of order $1/U$) to the energy levels if the spin wavefunctions are chosen as eigenfunctions of the Heisenberg chain.

3. Momentum distribution at finite doping

As a first application to the previous formulae, let us evaluate the one-particle density matrix $\rho(r)$ of the L-site $U \to \infty$ Hubbard chain at arbitrary filling $\rho = N/L$:

$$\rho(r) = \langle c^\dagger_{r,\uparrow} c_{0,\uparrow} \rangle. \tag{3.1}$$

The formal expression has been given by Ogata and Shiba [9] and is a direct consequence of the factorized form of the wavefunction (2.2): we notice that the annihilation of a real spin-up electron at the site 0 corresponds to the annihilation of a holon (i.e. a spinless fermion in equation (2.2)) at site 0 and to the removal of a spin-up in the spin wavefunction at the 'site' $j_0 = 0$ of the squeezed chain. Notice that, after this operation, the number of sites of the squeezed chain changes from N to $N-1$. Analogously, the creation of a spin-up electron at site r is split into two distinct operations: the creation of a holon at the same site in the physical chain and the creation of a spin up between the sites j and $j+1$ of the squeezed chain which now recovers the original N sites. Here j is the number of electrons within

the interval $(0, r)$ in the particular configuration we are considering. Therefore, in order to calculate the momentum distribution, we have to take the following steps.

(i) Select all configurations with a fixed number (say j) of electrons in the interval $(0, r)$.

(ii) Then proceed to the evaluation of the density matrix of the spinless fermion state in this subspace:

$$H_r(j) = \langle \psi_{SF} | c_r^\dagger \delta(N_r - j) c_0 | \psi_{SF} \rangle. \tag{3.2}$$

Here $N_r = \sum_{l=0}^{r} n_l$, the number operator in the interval $[0, r]$.

(iii) Move the spin-up (which must be present at the origin of the squeezed Heisenberg ring) to the jth site without introducing any phase factor. The latter step gives the contribution [9]

$$\Omega(j) = \tfrac{1}{2} \langle \phi_H | (2\boldsymbol{S}_j \cdot \boldsymbol{S}_{j-1} + \tfrac{1}{2}) \ldots (2\boldsymbol{S}_1 \cdot \boldsymbol{S}_0 + \tfrac{1}{2}) | \phi_H \rangle \tag{3.3}$$

where we have used the fact that $(2\boldsymbol{S}_i \cdot \boldsymbol{S}_{i-1} + \frac{1}{2})$ is the operator which permutes the spin at site i with that at site $i-1$. Therefore, each subspace of fixed j gives an independent contribution to the density matrix of the Hubbard chain whose final expression is obtained by summing the terms corresponding to all possible subspaces labelled by j:

$$\rho(r) = \sum_{j=0}^{r} \Omega(j)\, H_r(j). \tag{3.4}$$

In the following we will not carry out a rigorous evaluation of the two functions $H_r(j)$ and $\Omega(j)$ but, instead, we will just sketch the calculation of the long-distance behaviour of the charge part $H_r(j)$, which can be done in a straightforward (although lengthy) way. An analogous treatment of the spin term $\Omega(j)$ is much more difficult because it involves the evaluation of the many-particle correlation function (3.3) on a strongly correlated state. In fact, the interesting choice of $|\phi_H\rangle$ obviously corresponds to the ground state of the Heisenberg model which is given by the quite involved Bethe ansatz wavefunction. Exact results can be easily obtained only for small values of j. In fact, besides the obvious result $\Omega(0) = 1$, the exact value at $j = 1$ can also be obtained starting from the knowledge of the ground state energy of the Heisenberg model:

$$\Omega(1) = \langle 2\boldsymbol{S}_0 \cdot \boldsymbol{S}_1 + \tfrac{1}{2} \rangle_H = 1 - 2 \ln 2. \tag{3.5}$$

However these results are not of direct interest for the evaluation of the asymptotic behaviour of the density matrix because we expect that the relevant terms in the sum (3.4) are around $j \sim \rho r \gg 1$. In the following we will simply assume that the leading long-distance form of $\Omega(j)$ can be written as the product of the rapidly oscillating part of wavelength λ and the overall smooth function $h(j)$:

$$\Omega(j) = \mathrm{Re}(A \exp(\mathrm{i} 2\pi j/\lambda)) h(j) \tag{3.6}$$

where A is an undetermined complex constant. The precise form of $h(j)$ and the value of λ will be found indirectly by showing that there is a unique choice of λ and

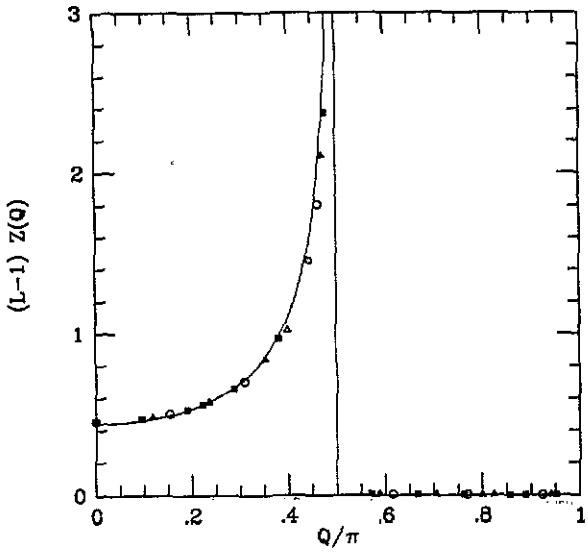

Figure 1. Quasiparticle weight $Z(Q)$ (equation (7)) for Heisenberg rings ranging from 6 to 22 sites: symbols, diagonalization results; full curve, fit to the data.

$h(j)$ consistent with the known singularity [7–11] of the momentum distribution near the Fermi wavevector.

In order to evaluate the long-distance behaviour of the charge part, we notice that the sign of $H_r(j)$ can be determined performing a Wigner–Jordan transformation on the free spinless fermion gas. In fact, the positivity of the hard-core boson ground state, implies that $H_r(j) = (-)^j P_r(j)$ where $P_r(j)$ is a positive definite function. Therefore $P_r(j)$ can be interpreted as a probability function and the calculation of $\rho(r)$ is formally quite similar to that of the spin–spin correlation function [10]. Following the same procedure and using the asymptotic expression (3.6), we end up with the following large distance form of the density matrix:

$$\rho(r) \sim h(\rho r)\,\mathrm{Re}\,C_r(2\pi/\lambda) \tag{3.7}$$

where $\rho = N/L$ is the mean density and

$$C_r(q) = \sum_{j=0}^{r-1} \mathrm{e}^{-\mathrm{i}qj} H_r(j). \tag{3.8}$$

The asymptotic behaviour of equation (3.8) for large distances can be calculated by taking its continuum limit. As shown in appendix A, the calculation is most conveniently done in the formalism of Mattis and Lieb [17] with the result:

$$C_r(q) \sim \{B_1 \mathrm{e}^{\mathrm{i}(q-\pi)\rho r} r^{-(1+(q^2/2\pi^2)-(q/\pi))} + B_2 \mathrm{e}^{\mathrm{i}(q+\pi)\rho r} r^{-(1+(q^2/2\pi^2)+(q/\pi))}\}. \tag{3.9}$$

This expression, together with (3.7), gives an oscillatory behaviour to the density matrix at wavevector $k = \rho((2\pi/\lambda) \pm \pi)$. In order to reproduce the expected $k_F = \rho\pi/2$ singularity of the momentum distribution, we must have $\lambda = 4$. The known

exponent of such a singularity $\theta = \frac{1}{8}$ is also reproduced if the smooth function $h(j)$ has a power-law decay of the form $h(j) \sim j^{-1/2}$. These consistency requirements allow the indirect evaluation of the spin term $\Omega(j)$ which will be crucial for the understanding of the hole dynamics in section 4. The asymptotic behaviour of the spin term derived from this calculation is, therefore,

$$\Omega(j) \underset{j\to\infty}{\longrightarrow} \frac{\mathrm{Re}[A \exp(\mathrm{i}\pi j/2)]}{\sqrt{j}}. \tag{3.10}$$

This expression is consistent with the exact diagonalization results from Ogata and Shiba [9] on a 26-site Heisenberg ring. Further numerical evidence is shown in figure 1 where the Fourier transform $Z(Q)$ of $\Omega(j)$ (see equation (4.21)) is plotted for Heisenberg rings of several sizes, ranging from 6 to 22 sites. Equation (3.10) would imply a singularity of $Z(Q)$ at $Q = \pm\pi/2$ of the form:

$$Z(Q) \underset{Q\to\pm\pi/2}{\longrightarrow} \frac{\text{constant}}{\sqrt{|Q \pm \pi/2|}} \frac{1}{L}. \tag{3.11}$$

However, exactly at $Q = \pi/2$ instead, $Z(Q)$ has a much slower decay:

$$Z(Q = \pm\pi/2) \sim L^{-1/2}. \tag{3.12}$$

A fit to diagonalization data, consistent with equation (3.11), is also shown in figure 1 substantiating the previous asymptotic behaviour (3.10).

Inserting equation (3.10) into equation (3.6) we get the final result for the density matrix:

$$\rho(r) \sim B_1 r^{-1/8} \frac{\cos(k_F r)}{r} + B_2 r^{-9/8} \frac{\cos(3k_F r)}{r} \tag{3.13}$$

which implies the presence of a subleading $3k_F$ singularity in the momentum distribution with exponent $\theta = \frac{9}{8}$. Such a singularity was first proposed [9] on the basis of accurate numerical computations and later justified on theoretical grounds by use of conformal invariance [12] and diagrammatic methods [13]. The present calculations shows that the feature at $3k_F$ is intimately related to the leading (i.e. k_F) singularity and originates from the same mechanism involving both the structure of the charge and that of the spin part of the wavefunction.

The decoupling between charge and spin, implicit in equation (2.2) gives information about the role of the spin degrees of freedom in the determination of the singularity in the momentum distribution. Note that every Fourier component of the charge part $C_r(q)$ is characterized by a different exponent in equation (3.9) which varies continuously with q. On the other hand, the antiferromagnetic spin ordering selects the particular wavelength $\lambda = 4$, picking up only one Fourier component of this function and leading to the simple power-law behaviour (3.13).

4. One-hole Green function

The dynamical properties of one hole in the $U \to \infty$ Hubbard model are described by the one-hole (spin-up) Green function;

$$G(k,\omega) = \langle \psi^0 | c^{\dagger}_{k,\uparrow} (\omega + E_0 - H - \mathrm{i}\delta)^{-1} c_{k,\uparrow} | \psi^0 \rangle \tag{4.1}$$

where ψ^0 is the non-degenerate ground-state wavefunction (of zero total momentum) of the undoped system and E_0 is its energy. Note that, since the half-filled ground state is a singlet, the one-hole Green function does not depend on the spin indices. Therefore we can focus our analysis on the spin-up component of the Green function.

In the following we use the Lehmann representation [18] of G:

$$G(k,\omega) = \int_{-\infty}^{\infty} d\omega' \frac{A(k,\omega')}{\omega - \omega' - i\delta} \tag{4.2}$$

where the spectral weight $A(k,\omega)$ is defined as

$$A(k,\omega) = \frac{1}{\pi} \operatorname{Im} G(k,\omega) = \sum_s |\langle \psi_s^h | c_{k,\uparrow} | \psi^0 \rangle|^2 \delta(\omega - E_s) \tag{4.3}$$

and $|\psi_s^h\rangle$ is a complete set of eigenfunctions of the $U \to \infty$ Hubbard model with one-hole. Here and in the following, energies are referred to the half-filled ground-state energy.

The energy spectrum and the degeneracy of the states at half-filling and in the case of one-hole immediately follow from equation (2.5): At half-filling ($N = L$) and $U = \infty$, the ground state has $E_0 = 0$ and is highly degenerate. The charge part ψ_{SF} of the wavefunction is just a constant while any spin configuration ϕ_H is allowed. Brinkman and Rice found the exact one-hole Green function for a particular choice of ϕ_H: a Néel spin background, which does not include quantum fluctuations. However this choice of spin state is not fully satisfactory because the degeneracy of the Hubbard ground state is lifted as soon as U is finite, the long-range order is destroyed and spin correlations are described by the ground state of the Heisenberg chain. In order to understand the role of spin fluctuations in the characterization of hole dynamics, we will compare two choices for ϕ_H: Néel and Heisenberg states.

The energy and the wavefunction of the generic one hole eigenstate at $U = \infty$ are slight generalizations of the ground-state results (2.4), (2.5). In particular, in an $L = 4n + 2$ ring, the spinless fermion wavefunction is a Slater determinant of plane wave states characterized by the set of $L - 1$ wavevectors:

$$k_j = 1/L(2\pi j + Q) \tag{4.4}$$

where j is an integer belonging to the interval $[-(L/2),(L/2-1)]$ and the phase shift Q is an integer multiple of $2\pi/(L-1)$ and coincides with the total momentum of the corresponding Heisenberg wavefunction ϕ_H in equation (2.2). Therefore Q can be considered as the 'spinon' momentum, relative to the half-filled system. The total momentum k of the state is related to the position of the (unique) 'hole' k_h in the $\{k_j\}$ distribution by

$$k = \sum_{k_j \neq k_h} k_j = (Q - \pi) - k_h. \tag{4.5}$$

The latter equation can be interpreted as a momentum conservation rule for the two elementary excitations. The energy spectrum of one hole is given by $E_s = -2\sum_{k_i \neq k_h} \cos(k_i)$ which can also be expressed in terms of the holon momentum:

$$E_{k,Q} = 2\cos k_h = -2\cos(k - Q). \tag{4.6}$$

According to equation (4.6), the energy spectrum only depends on the holon momentum. This result is valid just precisely at $U = \infty$: At finite, large U, a non-zero superexchange coupling $J = 4/U$ appears and a contribution

$$\epsilon_s(Q) = J((\pi/2)\cos Q + 2\ln 2) \tag{4.7}$$

has to be added to equation (4.6) besides a term $-J \ln 2 \cos(2k_h)$ coming from a three-site interaction. The precise form of this energy shift comes from the expectation value of the Hubbard Hamiltonian $\langle H \rangle$ at strong coupling on the state (2.2). Following [9], $\langle H \rangle$ can be related to the density correlation function of a spinless fermion gas and to the ground-state energy of the Heisenberg ring of $N = L - 1$ sites, with momentum Q:

$$\langle H \rangle = -2\cos(k_h) + LJ\langle \phi_H | S_0 \cdot S_1 - \tfrac{1}{4} | \phi_H \rangle \langle \psi_{SF} | n_0 n_1 | \psi_{SF} \rangle + \langle \text{three-site} \rangle \tag{4.8}$$

The charge factor in the previous expression can be easily evaluated using the fact that $\langle \psi_{SF} | n_0 n_1 | \psi_{SF} \rangle = 1 - 2/L$. The spin energy per site of an odd chain can be calculated by solving the Bethe ansatz equations for large size [19]

$$\langle \phi_H | S_0 \cdot S_1 - \tfrac{1}{4} | \phi_H \rangle = -\ln 2 + (\pi/2L)\cos Q + o(1/L)$$

with $-(\pi/2) \leqslant Q \leqslant (\pi/2)$. Analogously the three-site term contribution involves [9] a different spinless fermion correlation function

$$\langle \psi_{SF} | n_0 c^\dagger_{\pm 1} c_{\mp 1} | \psi_{SF} \rangle = -e^{\pm i 2k_h/L} + o(1/L).$$

Collecting all these terms we get the previously mentioned results for the excitation spectrum at first order in J. It is noticeable that an analogous calculation exact for $J = 2$ [19] gives exactly the same Q-dependence for the spinon excitation. In fact even in this case, as a consequence of spin–charge decoupling the energy can be written as a sum of a spin ϵ_s and a charge ϵ_h contribution:

$$E_{k,Q} = \epsilon_h(k_h) + \epsilon_s(Q) \tag{4.9}$$

where ϵ_s coincides with our perturbative result for $J = 2$ (the numerical factors in front of $\cos Q$ become identical at this J value). This suggests that our calculation for the spin excitations has a general validity beyond the perturbative regime.

In order to proceed to the determination of the spectral function $A(k,\omega)$, the generic matrix element appearing in equation (4.3) has to be evaluated. Clearly, the one-hole state $|\psi^h_s\rangle = \psi^{1h}_{SF} \cdot \phi^{1h}_H$ must have total momentum k, the state $|\psi^0\rangle$ having zero momentum. By performing a Fourier transform on $c_{k,1}$, we get

$$\langle \psi^h_s(k) | c_{k,\uparrow} | \psi^0 \rangle = \sqrt{L} \langle \psi^h_s(k) | c_{x=0,\uparrow} | \psi^0 \rangle \tag{4.10}$$

where an arbitrary site has been chosen as the origin of the chain. Now we are ready to exploit the (real space) factorization property of the $U \to \infty$ limit wavefunction (equation (2.2)). As usual, the annihilation of a spin-up electron at site $x = 0$ gives rise to the annihilation of a holon at the same site and to the removal of the spin

at the origin of the corresponding Heisenberg chain. Therefore the real space matrix element factorizes:

$$\langle \psi_s^h(k)|c_{x=0,\uparrow}|\psi^0\rangle = \langle \psi_{SF}^{1h}|c_{x=0}|\psi_{SF}^0\rangle \sigma_0. \tag{4.11}$$

The explicit evaluation of the charge part is straightforward and gives:

$$\langle \psi_{SF}^{1h}|c_{x=0}|\psi_{SF}^0\rangle = 1/\sqrt{L} \tag{4.12}$$

while the calculation of the spin part (σ_0) is much more complicated due to the structure of the Bethe ansatz Heisenberg wavefunction. Formally it can be written as

$$\sigma_0 = \langle L-1, -\tfrac{1}{2}|S_{x=0}^-|L,0\rangle_H \tag{4.13}$$

where the state $|L,m\rangle_H$ represents an eigenstate of the Heisenberg Hamiltonian on an L-site ring with total magnetization m. The matrix element (4.13) must be interpreted as the overlap between the state of the L-site chain obtained by flipping the spin-up at the origin, and the state of the L-site chain with a fixed spin-down at the origin while the spins on the other $(L-1)$-sites are distributed according to the amplitude $|L-1,-\frac{1}{2}\rangle$.

If this factorization is used for the evaluation of the spectral weight (4.3), we immediately obtain

$$A(k,\omega) = \sum_Q Z(Q)\delta(\omega - E_{k,Q}) \tag{4.14}$$

where the energy levels $E_{k,Q}$ are given by equation (4.6) and the quasiparticle weight $Z(Q)$ is formally given by

$$Z(Q) = \sum_s |\sigma_0|^2. \tag{4.15}$$

The sum in equation (4.15) runs over all the eigenstates $|L-1,-\frac{1}{2}\rangle$ of the Heisenberg chain of fixed total momentum Q. In fact, the momentum and frequency arguments (k,ω) in the spectral function fix the holon momentum k_h and the phase shift Q via equation (4.6). The fact that the sum (4.15) runs over a large subspace of states simplifies the calculation allowing for a formal resummation of (4.15). Using the completeness of the $|L-1,-\frac{1}{2}\rangle$ states in the subspace of fixed momentum Q and introducing the projector $\mathcal{P}_Q^{L-1}$ onto the subspace of total momentum Q of the $(L-1)$-site Heisenberg ring, equation (4.15) becomes

$$Z(Q) = \langle 0, L|S_{x=0}^+ \mathcal{P}_Q^{L-1} S_{x=0}^-|L,0\rangle_H. \tag{4.16}$$

The two operators S^+ and S^- can be easily eliminated by noting that $S_{x=0}^-$ commutes with the projector operator $\mathcal{P}_Q^{L-1}$ and that the Heisenberg ground state is a singlet†.

$$Z(Q) = \tfrac{1}{2}\langle 0, L|\mathcal{P}_Q^{L-1}|L,0\rangle_H. \tag{4.17}$$

† This expression is also valid in the case of a Néel state although it is not a spin singlet.

By definition, the projector $\mathcal{P}_Q^{L-1}$ is related to the translation operator $T_{(1,L-1)}$ on an $(L-1)$-site ring, which must be interpreted as the original L-site ring without the site at $x = 0$.

$$\mathcal{P}_Q^{L-1} = \frac{1}{L-1} \sum_{j=0}^{L-2} e^{-iQj} T_{(1,L-1)}^j. \tag{4.18}$$

The explicit expression for the translation operator $T_{(1,L-1)}$ in terms of spin operators is

$$T_{(1,L-1)} = (2\boldsymbol{S}_1 \cdot \boldsymbol{S}_{L-1} + \tfrac{1}{2}) \ldots (2\boldsymbol{S}_2 \cdot \boldsymbol{S}_1 + \tfrac{1}{2}). \tag{4.19}$$

This form can be further simplified by using the relation between the translation operators on the $(L-1)$-site and L-site rings:

$$(T_{(1,L-1)})^j = T_{(0,j)}(T_{(0,L-1)})^j \tag{4.20}$$

and $T_{(0,j)}$ is just the operator appearing in equation (3.3) as can be easily verified. Collecting all terms, the quasiparticle weight $Z(Q)$ (4.17) can be written as

$$Z(Q) = \frac{1}{2} \frac{1}{L-1} \sum_{j=0}^{L-2} (-1)^j e^{-iQj} \Omega(j). \tag{4.21}$$

The extra factor $(-1)^j$ comes from (4.20) and is a consequence of the finite total momentum ($P = \pi$) of the Heisenberg ground state on a $(4n+2)$-site ring. The function $\Omega(j)$ in equation (4.21) coincides with the one previously defined (equation (3.3))

$$\Omega(j) = \langle 0, L | T_{(0,j)} | L, 0 \rangle_H \tag{4.22}$$

whose long-range behaviour has been determined in section 3 (equation (3.10)).

It is interesting to compare the two equivalent expressions for $Z(Q)$ we have obtained: equations (4.15) and (4.21). In particular, the representation (4.15) suggests a physical interpretation of the oscillations we have previously found in $\Omega(j)$. Such oscillations can be related to the presence of a *spinon pseudo Fermi surface* located at $\pm\pi/2$. In order to clarify this statement, notice that, from the exact solution of the Heisenberg chain on a $4n+1$ ring [20], only one eigenfunction of fixed total momentum Q is characterized by real Bethe ansatz pseudo momenta k_j as long as $|Q| < \pi/2$. Instead, no real solution is present for $|Q| > \pi/2$. From a physical point of view, complex solutions are usually thought of representing collective modes not related to the elementary (i.e. one-particle) excitations of the system. Therefore it is expected that they are orthogonal (in the thermodynamic limit) to the state obtained by simply removing an electron, thereby giving no contribution to the quasiparticle weight $Z(Q)$. This would result in the vanishing of $Z(Q)$ outside the interval $|Q| < \pi/2$. This expectation is clearly confirmed by the diagonalization results of figure 1. These data also show that finite-size effects are not relevant for this quantity and the only singularity in $Z(Q)$ occurs at $Q = \pm\pi/2$ in agreement with our argument. Due to equation (4.21), this singularity of $Z(Q)$ at $Q = \pm\pi/2$ gives rise precisely the long-range oscillations in $\Omega(j)$ which have been found in section 3.

The expression of the spectral weight (4.14) is valid for a finite system. In the thermodynamic limit, the fine structure of the energy levels is washed out and $A(k,\omega)$ is not a collection of Dirac delta functions any more. Mathematically this corresponds to a coarse graining over the energy levels [18] in a small energy interval around ω:

$$A(k,\omega) \to \lim_{\delta \to 0} \left[\frac{1}{\delta} \int_{\omega}^{\omega+\delta} d\omega' A(k,\omega') \right] \tag{4.23}$$

which gives

$$A(k,\omega) = (L-1)[Z(Q_+(k,\omega)) + Z(Q_-(k,\omega))]N(\omega). \tag{4.24}$$

Here $Q_\pm(k,\omega) = k \pm \arccos(-\omega/2)$ and $N(\omega)$ coincides with the holon density of states:

$$N(\omega) = \frac{1}{2\pi} \frac{1}{\sqrt{4-\omega^2}}. \tag{4.25}$$

The spectral weight $A(k,\omega)$ can now be expressed, quite generally, in terms of $\Omega(j)$ by use of equation (4.21). The real space Green function then follows from the inverse Fourier transform of equation (4.2). With our choice (4.1) of the path in the complex ω plane, the Green function vanishes for $t < 0$ while for $t > 0$ is given by

$$G(r,t) = \tfrac{1}{2}\Omega(r) \exp(i\pi(r+1)/2) J_r(2t) \tag{4.26}$$

where J_r is the Bessel function of order r. Again, the frequency dependence of $G(r,\omega)$ is explicitly given by the Fourier transform of (4.26) independent of $\Omega(j)$. For every $r \geqslant 0$ the result is

$$G(r,\omega) = \frac{i}{2}\Omega(r) \frac{\exp(ir \arccos(\omega/2))}{\sqrt{4-\omega^2}} \tag{4.27}$$

for $\omega^2 < 4$, and

$$G(r,\omega) = \frac{1}{2}(\operatorname{sgn}\omega)^{r+1}\Omega(r)(\omega^2-4)^{-1/2}\left[\frac{|\omega|}{2} + \sqrt{(\frac{\omega}{2})^2 - 1}\right]^{-r} \tag{4.28}$$

for $\omega^2 > 4$.

Up to this point, we have not used any specific property of the Heisenberg ground state whose structure only enters the Green function through the function $\Omega(j)$. Therefore, equations (4.26)–(4.28) are valid for a wide class of spin states provided the appropriate function $\Omega(j)$ (3.3) is used. For instance, in the case of the Néel state $\Omega(j)$ can be easily computed:

$$\Omega(j) = \delta_{j,0} \qquad \text{(Néel)}. \tag{4.29}$$

This result, when substituted into equation (4.27), gives rise to the well known BR expression:

$$G(k,\omega) = 1/2\sqrt{\omega^2-4}. \tag{4.30}$$

This form of the Green function has several peculiar features:

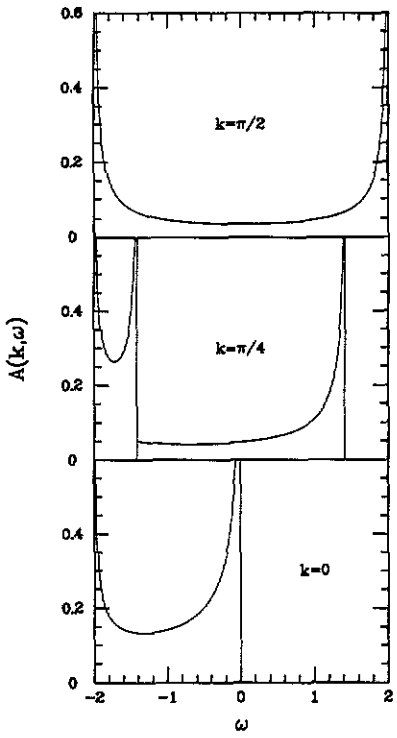

Figure 2. Spectral weight in the thermodynamic limit as a function of ω for different momenta k.

(i) It is completely incoherent with edge singularities at $\omega = \pm 2$.

(ii) It is independent of k showing that the hopping of the hole is inhibited by the (rigid) antiferromagnetic order.

However it is not clear whether these results are modified by quantum fluctuations in the spin background or, in other words, by scattering with spin excitations.

In the case of the Heisenberg ground state, the knowledge of $\Omega(0)$ ($\Omega(0) = 1$) allows the calculations of the on-site real-space Green function (density of states) which coincides with the general result of BR:

$$G(x = 0, \omega) = \tfrac{1}{2}\sqrt{\omega^2 - 4} \tag{4.31}$$

while $\Omega(1)$ (equation (3.5)) gives an exact expression for the Green function at nearest neighbours. For large distances, the asymptotic result (3.10) can instead be used in equations (4.26)–(4.28). More interestingly, equation (3.11) implies that the quasiparticle weight $Z(Q)$ always vanishes in the thermodynamic limit preventing the formation of a quasiparticle peak (i.e. a pole) in the hole Green function. This has to be contrasted with the conventional picture of a band insulator which is shown to be violated by the one-dimensional Hubbard model at half-filling. However, the divergence of $Z(Q)$ at $Q = \pm\pi/2$ (equation (3.11)) gives rise to branch cut singularities in the Green function at

$$\omega(k) = \pm 2 \sin k. \tag{4.32}$$

Around this line of singularities, the spectral weight behaves as

$$A(k,\omega) \sim |\omega - \omega(k)|^{-1/2} \tag{4.33}$$

except at $k = k_F = \pm\pi/2$ where

$$A(k = \pm\pi/2, \omega) \sim (2 - |\omega|)^{-3/4} \tag{4.34}$$

while the general structure of the spectral weight for the low-lying excitations ($k \sim \pm\pi/2\omega \sim -2$) has the unusual scaling form

$$A(k,\omega) \sim [|k \pm \pi/2|(2+\omega) + (2+\omega)^{3/2}]^{-1/2}. \tag{4.35}$$

A plot of the spectral weight for selected values of the momentum k is presented in figure 2 where a fit to the numerical data of $Z(Q)$ in small clusters has been used. More precisely, we have considered a simple analytical representation for the thermodynamic limit of $(L-1)Z(Q)$ consistent with the asymptotic behaviour (3.11):

$$(L-1)Z(Q) = \begin{cases} A + B/\sqrt{\cos Q} & \text{for } |Q| < \pi/2 \\ 0 & \text{for } |Q| > \pi/2 \end{cases} \tag{4.36}$$

where the parameters $A = -0.393$ and $B = 0.835$ have been analytically determined via equation (4.21) by use of the exact results $\Omega(0) = 1$ and $\Omega(1) = 1 - 2\ln 2$ (equation (3.5)). As can be seen in figure 1 this approximate analytical representation accurately reproduces the exact value of the quasiparticle weight in small rings. Therefore equation (4.36) can be usefully applied to the evaluation of the thermodynamic limit of the spectral weight through equation (4.24).

We conclude this section with few remarks on the results previously obtained:

(i) The physical origin of the rich structure of the spectral weight shown in figure 2 can be attributed to the presence of a 'pseudo Fermi surface' for spin excitations. In particular, the bandwidth depends on k due to the vanishing of $Z(Q)$ for $|Q| > \pi/2$ which is the signature of the fermion character of spinons.

(ii) The finite-size scaling of the quasiparticle weight at the branch cut is characterized by the exponent $\frac{1}{2}$ (3.12) which gives a much larger weight compared with the generic point (k,ω) where $Z \sim 1/L$ (3.11). It is interesting that the finite-size exponent $(1/2)$ of Z at the branch cut coincides with that of the spectral weight $A(k,\omega)$ close to the branch cut, showing that the frequency departure from the line of singularities scales as $1/L$. Notice that the strongest singularity occurs at $k = k_F = \pi/2$. This particular value of the momentum is singled out by the oscillations in $\Omega(j)$ which reflect the scattering of spinons in a Heisenberg antiferromagnet. This may be considered as the last reminiscence of the Luttinger theorem in this system.

(iii) We have performed a perturbative calculation including a small superexchange J in the one-hole energy spectrum (see equation (4.7)). Although our results strictly refer to the $U \to \infty$ limit, the analytic structure of the Green function persists at finite (small) J with relevant changes only at the Fermi momentum. The main qualitative difference introduced by a finite superexchange is the presence of a linear term in the energy spectrum $E_{k,Q}$ corresponding to $k = k_F$ and $Q \sim \pi/2$. As a result, the (k-dependent) one-particle density of states $|(\mathrm{d}E_{k,Q}/\mathrm{d}Q)|^{-1}$ is always finite in the (k,ω) plane, the band edge singularity (4.25) being cut off at an energy $\sim 1/J$.

Following the same procedure as before, the resulting one-hole Green function is slightly modified for $k \neq \pm k_F$. In particular, the locations of the branch cut and band edges are shifted by terms of order J and all singularities previously discussed are now of the form $|\omega - \omega(k)|^{-1/2}$. Contrary to the $J = 0$ case, the exponent of the singularity remains the same at band edges ($k = \pm k_F$). However the prefactor of this singularity changes abruptly with k from $O(1)$ to $O(1/J)$.

Although the exact exponents of this singularity differ from those found by the available approximate theories, the basic physics is reproduced by a few approximate treatments and, in particular, the general property of vanishing quasiparticle weight in one-dimensional Mott insulators has also been derived in [1, 2]. However it is remarkable that a small superexchange J leads to a 'smoothing' of the k_F singularity, that in our approach comes from the linear spin–wave excitations and the spin–charge decoupling.

5. Quasiparticle weight at finite doping

Further information on the dynamical properties of the one-hole excitations at finite doping can be obtained by examining the size scaling of the quasiparticle weight Z at the bottom of the band and $k = k_F$. This programme has been carried out at half-filling in section 4 where the result $Z \propto L^{-1/2}$ has been obtained.

At finite density this calculation is involved and has been attempted by several authors . In the following we perform the evaluation of Z for N electrons in a L-site ring in the $U \to \infty$ limit. At density $\rho = N/L$, the Fermi momentum is $k_F = \pi/2\rho$ and the energy of the lowest charge excitation is

$$E_h = 2\cos(2k_F). \tag{5.1}$$

Analogously to what has been done in section 4 (see equation (4.11)), the quasiparticle weight can be factorized to a spin and a charge part:

$$Z(k_F, E_h) = L\langle 0, N|S^+_{x=0} P^{N-1}_{Q=\pi/2} S^-_{x=0}|N, 0\rangle_H |\langle \psi^{N-1}_{SF}|c_0|\psi^N_{SF}\rangle|^2. \tag{5.2}$$

The first term is identical to the one we have evaluated at half-filling and scales as $N^{-1/2}$ independently of lattice size. The calculation of the charge part is straightforward but lengthy and is sketched in appendix B. The final result is, at low density,

$$|\langle \psi^{N-1}_{SF}|c_0|\psi^N_{SF}\rangle|^2 = \frac{A^2}{L} N^{3/8} [\Gamma(\tfrac{3}{4})]^2 \tag{5.3}$$

with $A = 0.9039$, which gives

$$Z(k_F, E_h) \sim N^{-1/8}. \tag{5.4}$$

This result has to be contrasted with the quasiparticle weight of the single hole which vanishes much faster. The change in the exponent is due to the charge part which behaves very differently at half-filling and at finite density. In fact, at $\rho = 1$ the charge degrees of freedom are frozen, leading to a suppression of the charge matrix element.

6. Conclusions

In this work, an explicit expression for the one-hole Green function of the one-dimensional Hubbard model at $U \to \infty$ has been obtained. Our result reveals a rich structure in the (k,ω) plane: The absence of a quasiparticle peak has been confirmed by this calculation which also showed the presence of branch cuts at $\omega = \pm 2 \sin k$ besides the well known band edge singularities predicted by BR.

From the knowledge of the Green function, we can characterize the dynamical properties of one hole in a quantum antiferromagnet. Quantum fluctuations in the spin degrees of freedom allow the propagation of the hole contrary to the case of a Néel background where the hole cannot propagate. This effect can be interpreted as a consequence of spinon scattering. However, this kind of hole motion is quite different from a free propagation due to the power-law behaviour of the hole Green function which results from the present calculation. Therefore the one-dimensional quantum antiferromagnet is not a conventional insulator but shows peculiar features which might be generic for Mott insulators. Most of the anomalous properties we have found, derive from the occurrence of spin–charge decoupling (4.5) (4.9) which, in principle, can be generalized in more than one dimension.

Although our calculation strictly refers to the $U \to \infty$ limit, the analytic structure of the Green function persists at finite (small) J with only minor changes at least for $k \neq k_F$. It is surprising that a finite superexchange coupling leads to the weakening of the strong band edge singularity at $k = \pm k_F$ present for $J = 0$. This is due both to the occurrence of spin–charge decoupling and to the linear dispersion of the spin-wave excitations.

We have also calculated the quasiparticle weight Z for one hole in the half-filled Hubbard model and at finite doping. In both cases Z approaches zero as a power law when the size of the system is increased. The corresponding exponents coincide with those characterizing the singularities of the Green function away from the band edges. We believe that this is a general feature of the Green function in any dimension: if Z saturates to a constant value we would have either a conventional band insulator or a Fermi liquid, while a vanishing Z for the lowest excitation is the signature of a non-Fermi liquid behaviour. This property can be useful for numerical investigations of the nature of the quasiparticle excitations in strongly correlated electron systems.

Recent numerical computations of the Green function [23] of the t–J model on finite systems have been unable to detect the branch cut feature we have obtained from the Bethe ansatz solution of the Hubbard model. This is probably due to the smallness of the clusters which have been considered. However, a peak at approximately $\omega = 2 \sin k$ seems to be present in the published data.

The problem we have solved (i.e. the evaluation of the Green function in a Mott insulator) is also important from an experimental point of view because the spectral function is directly related to photoemission experiments and it is clearly useful to know the predictions of a simple theoretical model on quantities of direct experimental interest. Besides, this is, to our knowledge, one of the first examples of fully microscopic calculations of the Green function for a non-trivial insulator.

Acknowledgments

We gratefully acknowledge stimulating discussions with M Rice and E Tosatti. One

of us (AP) is grateful to M Rice for kind hospitality at ETH during the early stages of this work.

Appendix A

In this appendix the quantity

$$C_r(q) = \langle \psi_{SF} | c_r^\dagger e^{iq \sum_{j=0}^{r-1} n_j} c_0 | \psi_{SF} \rangle \tag{A1}$$

is evaluated in the asymptotic limit $r \gg 1$.

As is well known [17] the large-distance behaviour of correlation functions of a spinless fermion ground state comes from the outmost electrons of ψ_{SF} with momentum close to $\pm k_F$. For a free spinless fermion state, the full Slater determinant $\psi_{SF} = \prod_{|k| \leq k_F} c_k^\dagger |0\rangle$ can be simplified by linearizing the band around $\pm k_F$. This gives rise to the two branches :

$$\begin{aligned} \psi_{+,k}^\dagger &= c_k^\dagger \qquad \text{for } k \sim k_F \\ \psi_{-,k}^\dagger &= c_k^\dagger \qquad \text{for } k \sim -k_F. \end{aligned} \tag{A2}$$

ψ_{SF} is the product of one-particle states in the two branches:

$$\psi_{SF} = \psi_{+,SF} * \psi_{-,SF} \tag{A3}$$

with

$$\psi_{\pm,SF} = \prod_{k \sim \pm k_F} c_k^\dagger |0\rangle. \tag{A4}$$

Moreover the density operator $N_r = \sum_{j=0}^{r-1} n_j$ appearing in (A1) splits up into the sum:

$$N_r = r\rho + \frac{1}{L} \sum_{p \neq 0} f_r(p)[\rho_+(p) + \rho_-(p)] \tag{A5}$$

where $\rho = N/L$ is the total density and $\rho_\pm(p)$ are density operators in the two different branches:

$$\rho_\pm(p) = \sum_k \psi_{k+p,\pm}^\dagger \psi_{k,\pm} \tag{A6}$$

and $f_r(p) = (1 - e^{-ipr})/(1 - e^{-ip})$. In the expression (A3) we have neglected less singular contribution ($p \sim 2k_F$) and all the sums should be restricted to the regions determined by (A2). However the wavevector components far from the important regions $k \sim \pm k_F$ do not affect the correlation functions at large distance. In this way

the momentum restriction in (A6) can be neglected and, in this case [17], the charge density fluctuations satisfy boson-like commutation relations:

$$\rho_+(p) = \left(\frac{pL}{2\pi}\right)^{1/2} b_p^\dagger \qquad \text{for } p > 0$$

$$\rho_-(p) = \left(\frac{-pL}{2\pi}\right)^{1/2} b_p^\dagger \qquad \text{for } p < 0 \tag{A7}$$

where $b_p^\dagger$ are the usual boson creation operators: $[b_p, b_{p'}^\dagger] = \delta_{p,p'}$.

Due to the factorization properties of the wavefunction ψ_{SF} (A3) and using the asymptotic expression for N_r (A5), $C_r(q)$ can be written in the following way:

$$C_r(q) = e^{iq\rho r}\{G_+(r)H_-(r) + G_-(r)H_+(r)\} \tag{A8}$$

where

$$G_\pm(r) = \langle \psi_{\pm,SF} | e^{iq/L \sum_{p>0} f_r(p)\rho_\pm(p)} | \psi_{\pm,SF}\rangle \tag{A9}$$

and

$$H_\pm(r) = \langle \psi_{\pm,SF} | \psi_{\pm,r}^\dagger e^{iq/L \sum_{p>0} f_r(p)\rho_\pm(p)} \psi_{\pm,0} | \psi_{\pm,SF}\rangle \tag{A10}$$

$G_\pm(r)$ can be easily evaluated by employing normal order in the right-hand side of equation (A9), i.e. using the commutation rules in (A7) and noting that

$$\rho_+(-p)|\psi_{+,SF}\rangle = 0 \qquad \text{and} \qquad \rho_-(p)|\psi_{-,SF}\rangle = 0 \qquad \text{for } p > 0. \tag{A11}$$

In this way we get

$$G_\pm(r) = \exp\left[-\frac{q^2}{2}\sum_{p>0}\frac{1}{L^2}\left(\frac{pL}{2\pi}\right) f_r(p) f_r(-p)\right] \to \text{constant } r^{-q^2/4\pi^2}. \tag{A12}$$

We note that the latter asymptotic result for $G_\pm(r)$ is in agreement with the exact result for $q = \pi$, when $G_\pm(r)$ becomes a Hilbert determinant [10].

The evaluation of $H_\pm(r)$ is more involved but almost identical to the calculation [17] of the density matrix by Mattis and Lieb. After normal ordering of the exponential factor in $H_\pm(r)$ we get

$$H_\pm(r) = G(r)\langle \psi_{\pm,SF} | \psi_{\pm,R}^\dagger W_C W_A \psi_{\pm,0} | \psi_{\pm,SF}\rangle \tag{A13}$$

where W_C, W_A contains only boson creation or annihilation operators respectively:

$$W_C = \exp\left[iq\int_0^L dx\, h_\pm(x) N_\pm(x)\right]$$

$$W_A = \exp\left[iq\int_0^L dx\, h_\mp(x) N_\pm(x)\right] \tag{A14}$$

with

$$h_{\pm}(x) = \frac{1}{L} \sum_{\pm p>0} e^{ipx} f_r(p) \tag{A15}$$

and the density operator are: $N_{\pm}(x) = (1/L) \sum_{p \neq 0} \rho_{\pm}(p) e^{-ipx}$. From these definitions:

$$\langle \psi_{\pm,SF} | (W_L)^{-1} = \langle \psi_{\pm,SF} | \qquad \text{and} \qquad (W_L)^{-1} | \psi_{\pm,SF} \rangle = | \psi_{\pm,SF} \rangle. \tag{A16}$$

Therefore the last factor in the right-hand side of equation (A13) can be easily evaluated:

$$\begin{aligned} &\langle \psi_{\pm,SF} | \psi^{\dagger}_{\pm,r} W_C W_A \psi_{\pm,0} | \psi_{\pm,SF} \rangle \\ &\quad = \langle \psi_{\pm,SF} | [(W_C)^{-1} \psi^{\dagger}_{\pm,r} W_C][W_A \psi_{\pm,0} (W_A)^{-1}] | \psi_{\pm,SF} \rangle \\ &\quad = e^{-iq[h_{\pm}(r) + h_{\mp}(0)]} \langle \psi_{\pm,SF} | \psi_{\pm,r} \psi_{\pm,0} | \psi_{\pm,SF} \rangle \\ &\quad = \text{constant } r^{-q/\pi} e^{\mp i k_F r} / r \end{aligned} \tag{A17}$$

where in the latter two equalities we have used [17]

$$\begin{aligned} (W_C)^{-1} \psi^{\dagger}_{\pm,r} W_C &= e^{-iq h_{\pm}(r)} \psi^{\dagger}_{\pm,r} \\ W_A \psi_{\pm,0} (W_A)^{-1} &= e^{-iq h_{\mp}(0)} \psi_{\pm,0} \end{aligned} \tag{A18}$$

and the asymptotic form of the free electron density matrix on the two different branches:

$$\langle \psi_{\pm,SF} | \psi^{\dagger}_{\pm,r} \psi_{\pm,0} | \psi_{\pm,SF} \rangle \to e^{\mp i k_F r} / r. \tag{A19}$$

Collecting the results (A14), (A15) and (A17) and inserting them into the expression for $C_r(q)$ (A9) we obtain the final result for $C_r(q)$ as quoted in the text (equation (3.9)).

Appendix B

In this appendix we sketch the calculation of the charge part of the quasiparticle weight equations (5.2) and (5.3) at finite doping. The matrix element which has to be evaluated, is

$$\langle c_0 \rangle_{SF} \equiv \langle \psi^{N-1}_{SF} | c_0 | \psi^{N}_{SF} \rangle \tag{B1}$$

where the states $|\psi^{N}_{SF}\rangle$ are the spinless fermion states entering the Bethe ansatz solution (2.2) for the ground state of N electrons in the $U \to \infty$ Hubbard model. The exact wavevectors characterizing the spinless fermion states are shown in equations (2.3)

and (2.4). By writing the annihilation operator at the origin c_0, in momentum space and using the orbitals defined by equation (2.3), we get

$$\langle c_0 \rangle_{SF} = \frac{1}{\sqrt{L}} \sum_{j=-2n-1}^{2n} (-1)^{j+1} \langle \psi_{SF}^{N-1} | \psi_{SF}^{N} \rangle_{j_h} \tag{B2}$$

the state $|\psi_{SF}^{N}\rangle_{j_h}$ is the Slater determinant built with the plane waves defined by equation (2.3) where the j_h orbital of the hole has been removed. Therefore the calculation of the charge matrix element is reduced to the evaluation of the overlap between two Slater determinants. Following [10] the overlap can be expressed as the determinant of a $(4n+1) \times (4n+1)$ matrix:

$$B_{j,l}^{(j_h)} = \frac{1}{L} \sum_{r=0}^{L-1} \exp\left(\frac{2\pi i}{L}(j-l+\delta)r\right) = (1-e^{2\pi i \delta})\left[1-\exp\left(\frac{2\pi i}{L}(j-l+\delta)\right)\right]^{-1} \tag{B3}$$

where the phase shift $\delta = \frac{1}{2} - n/(4n+1) - \frac{1}{4}$ and the indices run in the intervals $j \in [-2n-1, 2n]$ (but $j \neq j_h$) and $l \in [-2n, 2n]$. In order to proceed in the evaluation of the determinant of the matrix $B^{(j_h)}$ it is convenient to restrict the analysis to the low density limit $N/L \ll 1$ where the calculation can be performed exactly. It is known that the form (but not the prefactor) of the leading singularity is independent of density and therefore our result is actually more general than this derivation might suggest. By expanding to leading order the exponential in the denominator of equation (B3) we find

$$\det B^{(j_h)} = (-1)^n \det \left[\frac{\sin \pi\delta}{\pi} \frac{1}{j-l+\delta}\right]. \tag{B4}$$

In order to evaluate $\langle c_0 \rangle_{SF}$ it is useful to introduce an auxiliary Hilbert matrix of dimensions $(4n+2) \times (4n+2)$

$$H_{j,l} = \left[\frac{\sin \pi\delta}{\pi} \frac{1}{j-l+\delta}\right] \tag{B5}$$

where now both indices belong to the interval $[-2n-1, 2n]$.

The formal solution of the Wiener–Hopf problem defined by the matrix (B5)

$$H_{j,l} x_l = \delta_{j,-2n-1} \tag{B6}$$

can be obtained by Cramer's rule:

$$x_j = \frac{(-1)^{j+1}}{\det H} \det B^{(j)} \tag{B7}$$

which relates the quantity of interest ($\det B^{(j)}$) to the solution of the linear equation (B6) (x_j). Substituting this result into equation (B2) we arrive at a compact expression for the charge matrix element:

$$\langle c_0 \rangle_{SF} = \frac{(-1)^n}{\sqrt{L}} \det H \sum_{j=-2n-1}^{2n} x_j. \tag{B8}$$

The evaluation of the determinant of the Hilbert matrix H is straightforward [21] and gives for large $N = 4n + 2$:

$$\det H \to AN^{-\delta^2} \sim N^{1/16} \tag{B9}$$

where the prefactor A is given by

$$\ln A = -\delta^2(1+\gamma) + \sum_{l=1}^{\infty} l\left[\ln\left(1 - \frac{\delta^2}{l^2}\right) + \frac{\delta^2}{l^2}\right] \sim -0.10101 \tag{B10}$$

and $\gamma \sim 0.5772$ is the Euler constant. This calculation does not exhaust the evaluation of the charge matrix element because an important contribution also comes from the sum in equation (B8). The sum can be estimated noting that, from the definition (B6),

$$x_j = H^{-1}_{j,-2n-1} \tag{B11}$$

and the inverse of a Hilbert matrix can be explicitly evaluated [23]. The problem is then reduced to the calculation of the finite sum:

$$\sum_{j=-2n-1}^{2n} x_j = \frac{\Gamma(N+\delta)}{(N-1)!\,\Gamma(\delta)} \sum_{p=0}^{N-1} \frac{\Gamma(p+\delta)\,\Gamma(N-p-\delta)}{p!(N-1-p)!}. \tag{B12}$$

Using the integral representation of Euler's gamma function

$$\Gamma(z) = \int_0^{\infty} \mathrm{d}t\, \mathrm{e}^{-t} t^{z-1} \tag{B13}$$

(valid for $z > 0$) the sum can be performed analytically with the result

$$\sum_{p=0}^{N-1} \frac{\Gamma(p+\delta)\,\Gamma(N-p-\delta)}{p!(N-1-p)!} = \int_0^{\infty} \mathrm{d}t\, \frac{t^{\delta-1}}{t+1} = \Gamma(\delta)\Gamma(1-\delta). \tag{B14}$$

Collecting all terms together, the large-N asymptotic behaviour of the charge matrix element is

$$\langle c_0 \rangle_{\mathrm{SF}} \to \frac{(-1)^n}{\sqrt{L}} A\Gamma(1-\delta) N^{\delta-\delta^2} \tag{B15}$$

where $\delta = \frac{1}{4}$ and the prefactor $A \sim 0.9039$ in the low density limit. Notice that an important contribution ($\sim N^{\delta}$) to $\langle c_0 \rangle_{\mathrm{SF}}$ comes from the term in equation (B12) showing that the evaluation of the charge matrix element cannot be reduced to the term in equation (B9) which represents the overlap between two Slater determinants built with the orbitals (2.3) and (2.4), contrary to what is often claimed in the literature.

References

[1] Brinkman W F and Rice T M 1970 *Phys. Rev.* B **2** 1324
[2] Kane C L, Lee P A and Read M 1989 *Phys. Rev.* B **39** 6880
[3] Shraiman B I and Siggia E D 1990 *Phys. Rev.* B **42** 2485
[4] Joynt R 1988 *Phys. Rev.* B **37** 7979
[5] von Szczepanski K J, Horsch P, Stephan W and Ziegler M 1990 *Phys. Rev.* B **41** 2017
[6] Solyom J 1979 *Adv. Phys.* **28** 201
[7] Schulz H 1990 *Phys. Rev. Lett.* **64** 2831
[8] Anderson P W and Ren Y 1990 unpublished
[9] Ogata M and Shiba H 1990 *Phys. Rev.* B **41** 2326
[10] Parola A and Sorella S 1990 *Phys. Rev. Lett.* **64** 1831
[11] Parola A and Sorella S 1991 *Preprint* ETH-TH 81–5
[12] Frahm H and Korepin V E 1990 *Phys. Rev.* B **42** 10553; 1990 *Phys. Rev.* **41** 2017
[13] Penc K and Solyom J 1991 *Phys. Rev.* B **44** 12 690
[14] Sorella S, Parola A, Parrinello M and Tosatti E 1990 *Europhys. Lett.* **12** 721
[15] Caspers W J and Iske P L 1989 *Physica* A **157** 1033
[16] Lieb E H and Wu F Y 1968 *Phys. Rev. Lett.* **20** 1445
[17] Mattis D C and Lieb E H 1963 *J. Math. Phys.* **6** 304
[18] Fetter A L and Walecka J D 1971 *Quantum Theory of Many Particle Physics* (New York: McGraw-Hill)
[19] Bares P A, Blatter G and Ogata M 1991 *Phys. Rev.* B **44** 130
[20] Faddeev L D and Takhtajan L A 1981 *Phys. Lett.* **85A** 375
[21] Ziegler M and Horsch P 1990 *Proc. Nato Advanced Research Workshop on Dynamics of Magnetic Fluctuations in High Temperature Superconductors* ed G Reiter, P Horsch and G Psaltakis (New York: Plenum)
[22] McCoy B N and Wu T T 1973 *The Two Dimensional Ising Model* (Cambridge, MA: Harvard University Press)